Upper Cervical Spine Kinematic Response and Injury Prediction

Duane S. Cronin, Jason B. Fice, Jennifer A. DeWit, Jeff Moulton

Abstract The upper cervical spine comprising the base of the skull, first cervical vertebra (C1) and second cervical vertebra (C2) is one of the most complex joints in the human spine. In low severity automotive crash scenarios, ligament distraction has been implicated as a source of whiplash pain, while at higher impact severities vertebral fracture and distraction can lead to serious or fatal injuries. The objective of this study was to investigate kinematic response and predicted injury of the upper cervical spine using a 50th percentile male numerical model including detailed representations of the ligaments, vertebral bodies and joints. The model was evaluated in four modes of loading. In general, the model was able to predict failure loads and distractions for flexion, extension, tension and axial rotation in good agreement with the available experimental data. The failure load in tension was higher than the experimental average likely due to the younger ligament properties used, which were stiffer and stronger than properties from an older population.

Keywords Upper cervical spine, injury, finite element model.

I. INTRODUCTION

The upper cervical spine permits large ranges of motion in flexion, extension and rotation which are enabled by synovial joints, ligaments and musculature connected between the skull, first cervical vertebra or atlas (C1), and second cervical vertebra or axis (C2). This joint is important in the kinematic response of the head impact scenarios [1] but can be challenging to model due to the complex connectivity of the hard and soft tissues. In low severity automotive crash scenarios, ligament distraction has been implicated as a source of whiplash pain [2] in the upper cervical spine, while at higher impact severities vertebral fracture and distraction can lead to serious or fatal injuries depending on the impact location [3].

To investigate upper cervical spine response, this study used the upper cervical spine from a detailed 50th percentile male numerical model including detailed representations of the ligaments, vertebral bodies and joints (Fig. 1). The full model was previously validated using a hierarchical approach, beginning at the segment level in the lower cervical spine with physiological loads, followed by full spine impact scenarios (15 g frontal, 7 g lateral, 4 g rear impact [4]) which did not result in catastrophic tissue failure. The full spine model was found to generally agree with the cadaver studies at the segment level and the volunteer studies at the full spine level using ligament properties from the literature [1].

The objective of this study was to investigate upper cervical spine response and tissue failure using a functional spinal unit (FSU) model (skull, C1, C2) with ligament properties representative of a younger population. Recently, detailed mechanical properties of the craniovertebral ligaments have been experimentally measured for a younger population (average age 45 YO) at strain rates relevant to automotive crash scenarios [5]. The upper cervical spine model will contribute to the predictive capabilities of a full human body model to predict injury in automotive crash scenarios.

D.S. Cronin is an Associate Professor at the University of Waterloo, Canada in Mechanical Engineering (dscronin@uwaterloo.ca) (phone: 519-888-4567 x32682, fax: 519- email: dscronin@uwaterloo.ca) J.B. Fice, MASc, University of Waterloo, Canada, J.A DeWit, MASc, University of Waterloo, Canada, J. Moulton, MASc, University of Waterloo, Canada.

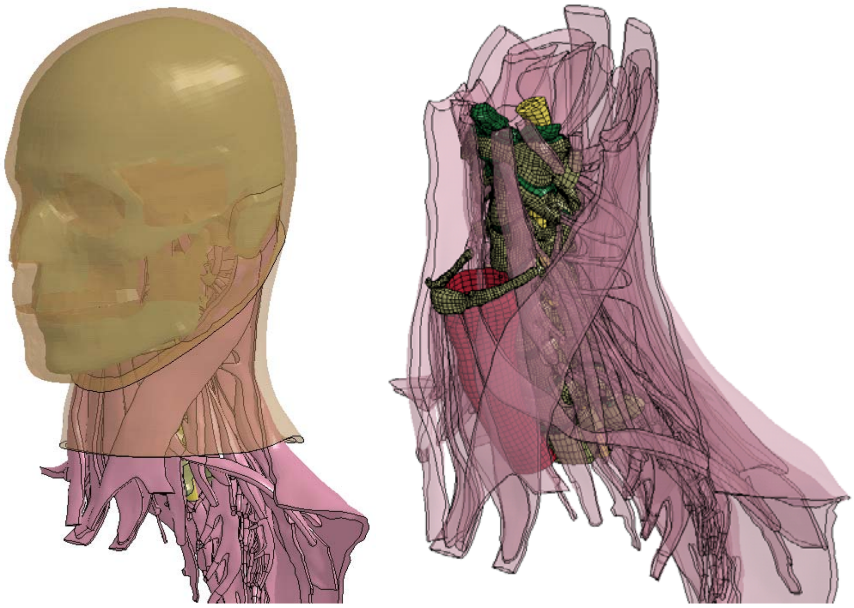

Fig. 1. Full cervical spine numerical model (Neck model and simplified head with translucent skin [L], neck model with translucent muscle [R])

II. METHODS

A numerical model of the cervical spine (Fig. 1) was developed from an approximately 50th percentile male subject (26 YO, 174.9 cm height, 78.6 ± 0.77 kg based on CT and MRI scan data [6]). The full cervical spine model [4] included all relevant hard and soft tissues with a total of 304,385 elements (204,180 solid elements, 95,630 shell elements and 4,575 axial elements). The structures relevant to the current study were extracted from the full model (Fig. 2) to be used for verification and validation of the mechanical and failure properties of the tissues. The vertebrae were meshed using solid elements for the cancellous bone and a layer of shell elements representing the cortical bone. The articular cartilage was modeled with solid elements. Each ligament was modeled with a series of axial elements to accurately distribute the load to the vertebral bodies, and to allow for progressive failure to predict post-ultimate response [7]. Failure was modeled by symmetric progressive erosion of axial elements to gradually reduce the stiffness of the ligament to zero from the distraction at ultimate load to the final failure distraction. Musculature was not considered in this study since the comparable experimental data were based on ligamentous functional spinal units loaded in tension, flexion, extension and axial rotation [8-10]. The density of the bone mesh was previously found to be suitable to predict stresses and the onset of failure or fracture in a similar detailed model of the lower cervical spine [7]. The functional spinal unit (Fig. 2) consisted of 12246 solid elements and 25800 shell elements representing the vertebrae and cartilage, and 293 axial elements representing the ligaments.

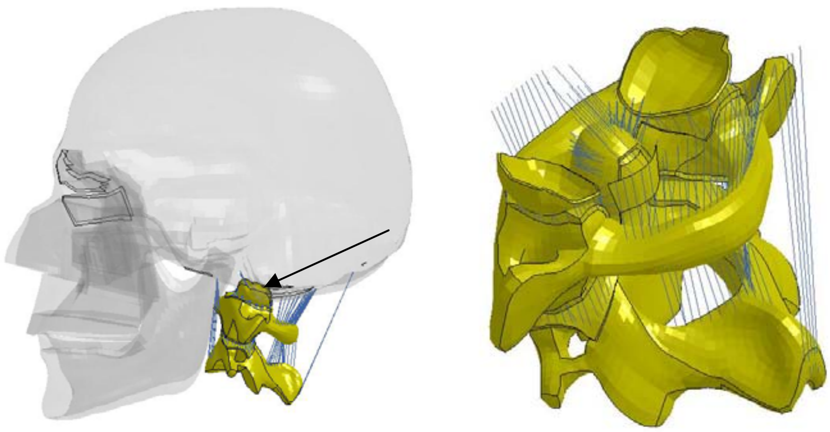

Fig. 2. Upper cervical spine [left] functional spinal unit (C0-C1-C2) [right]

Material Properties

The cortical bone was modeled with shell elements with a density of 2000 kg/m^3 and using mechanical properties measured by McElhaney [11]. The properties were implemented in an elastic-plastic material model where the modulus of elasticity (18.4 GPa) was determined through regression fitting the linear region, and the yield strength (189 MPa) was determined using the modulus and 0.2% offset method. The limited permanent deformation prior to failure, observable in the published data, was modeled using a tangent modulus and ultimate strain to failure (0.0178 mm/mm).

The cancellous bone was modeled with solid elements and was described using an elastic-plastic material model. The apparent density of the bone was 0.2 kg/m^3 while the balance of the material was assumed to have the density of water, for an overall density of 1100 kg/m^3. The elastic modulus (442 MPa) and yield strength (2.83 MPa) were defined as a function of the apparent density [12]. The ultimate strength was 5.5 MPa at a failure strain of 0.095 mm/mm [13].

For the purpose of this study, the simplified skull was modeled using rigid shell elements with the appropriate mass and inertia properties. The cartilage was modeled as viscoelastic using the mechanical properties as described and implemented by Panzer [1].

The mechanical properties for the upper cervical spine ligaments were taken from experimental measurements reported by Mattucci [5]. An example of the anterior atlanto-occipital membrane is shown in Fig. 3. Ligament failure was implemented with progressive failure of the axial elements [7] to model the post-ultimate response, which was essential to predict tissue failure and post-failure response.

Each ligament was modeled using multiple discrete axial elements (Fig. 3, right). The number of axial elements used to represent each ligament ranged from 3 to 40, corresponding to the physical size of the ligament and attachment, and was determined in part by the finite element mesh density of the vertebral bodies. The elements were evenly spaced along the length of each ligament (Fig. 2)

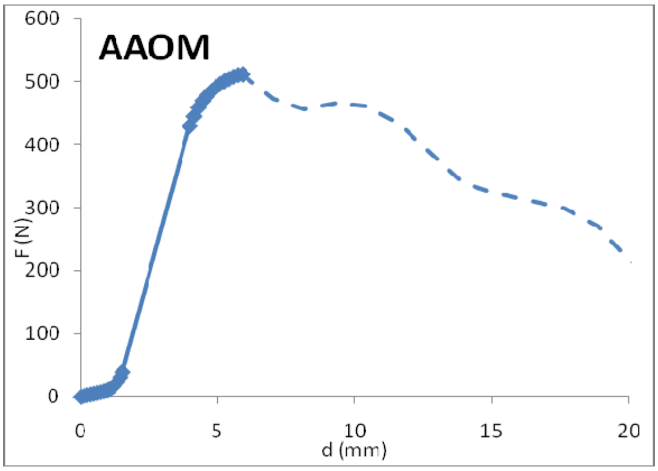

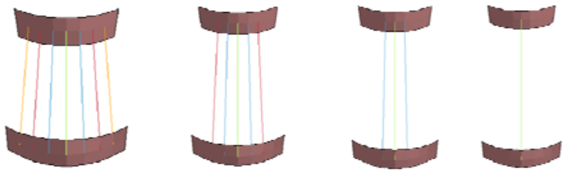

Fig. 3. Ligament mechanical properties [tectoral membrane complex, left] and progressive failure implementation [right]

Load Cases

Four load cases were considered including flexion [10], extension [10], tension [8] and axial rotation [9] using two different model implementations. The first model implementation included the as-measured ligament properties with failure response defined. The second model implementation included hard tissue failure prediction and laxity in some ligaments. In general, the skull was fixed at the head CG and displacement boundary conditions were applied to the inferior surface of the C2. The resulting load or moment was monitored during the simulation and the peak value along with the associated displacement or rotation was recorded. The individual tissues were investigated to determine if failure had occurred. Displacement control was used since this provided greater numerical stability, particularly when the failure load or moment was exceeded. For each load case, the first result presented included the as-measured ligament mechanical properties and progressive failure definition. The second model for each load case included hard tissue failure and laxity incorporated in some ligaments based on evaluation of the different load cases. The laxities were determined from a larger parametric investigation, not presented in detail in this study. The finite element models were solved using a commercial explicit finite element program (LS-Dyna 971 version 4.2.1, LSTC).

III. RESULTS

The predicted initial failure moment and rotation (Fig. 3) in flexion (36.4 Nm, 61.9°) for the model implementation with ligament failure was in good agreement with the experimental data (39 Nm, 58.7°), and demonstrated stiffness comparable to the one sample trace that was available. Ligament failure occurred first at the ISL, followed by the PAAM. Subsequently, the moment increased significantly as C1 contacted C2. When hard tissue failure was active, the predicted failure response (28.3 Nm, 63.6°) was outside the experimental corridor due to a predicted Type II odontoid fracture (2^{nd} peak in Fig. 3). Failure in the experiments was reported as failure of the ligaments (PAAM, PAOM) and, in some cases, a Type III odontoid fracture.

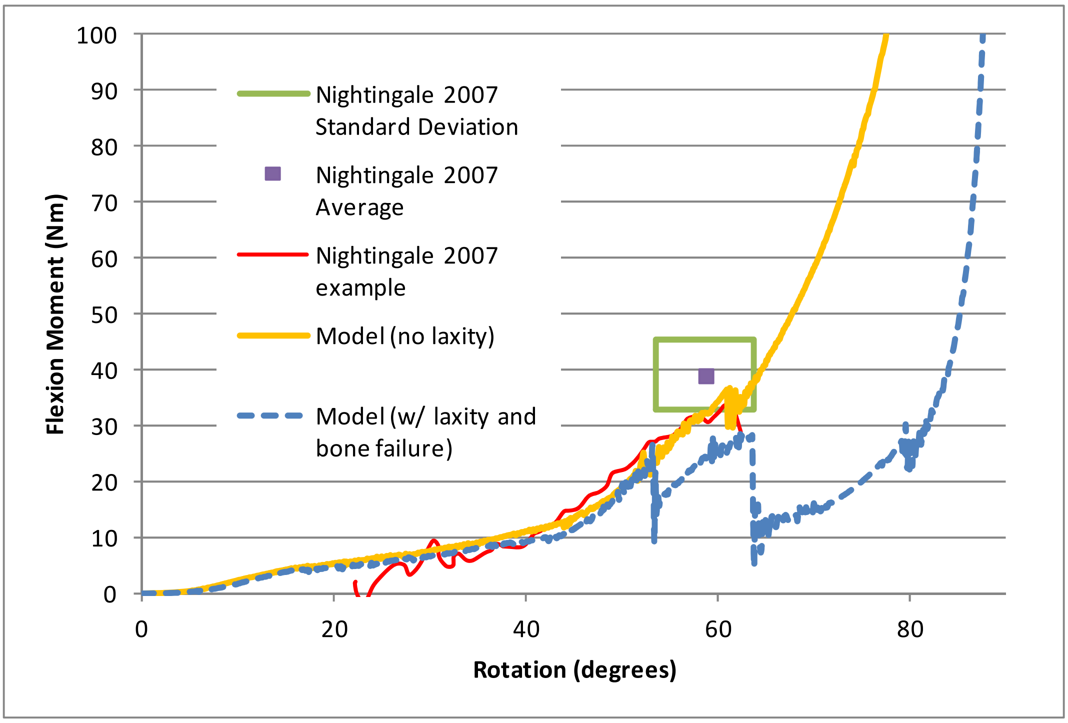

Fig. 3. Flexion moment-rotation

The onset of predicted failure in extension (33.3 Nm, 41.2°) (Fig. 4) for the model implementation with ligament failure was below the experimental average (49.5 Nm, 42.0°) but within the experimental corridor with failure initiating at the anterior atlanto-axial membrane (AAAM). The post-ultimate load ligament damage model allowed for continued distraction of the joint followed by a rapid increase after contact between the C1 and C2 vertebrae leading to an increased moment. When hard tissue failure was active and ligament laxity was included, the initial failure or first load peak (32.3 Nm, 44.4°) resulted from failure of the AAAM. This was followed by subsequent peaks as adjacent tissues failed and final fracture of the posterior arch (C1) and spinous process (C2). Failure in the experiments was reported as C1-C2 dislocation and some failures at the fixation were also noted.

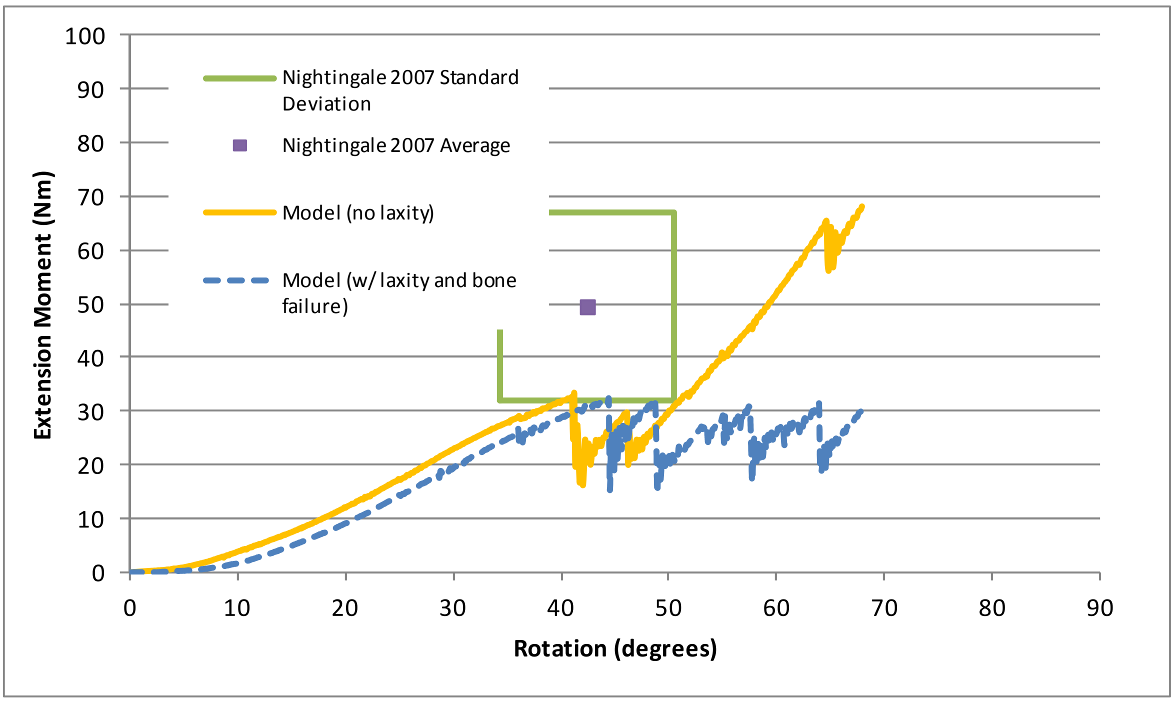

Fig. 4. Extension moment-rotation

The predicted tension failure load (Fig. 5) was similar for the case without ligament laxity (3.0 kN, 10.5 mm) and with laxity (2.9 kN 10.5 mm), being higher than the published average value (2.4 kN, 10.8 mm). Failure initiated at the AAAM.

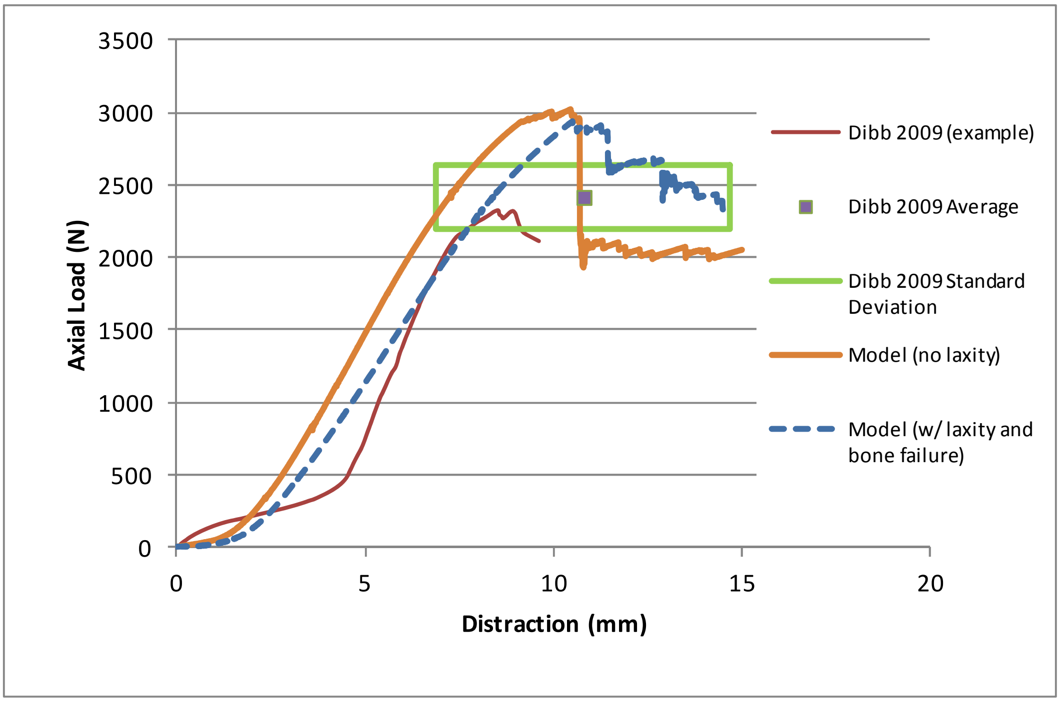

Fig. 5. Tension-displacement response

The failure torque under axial rotation (9.6 Nm, 51.9°) (Fig. 6) was lower than the average reported in the literature (13.6Nm, 68°), occurring by ligament failure and distraction of the C1-C2 joint. However, the predicted torque reached a plateau from approximately 50 to 70°, which was consistent with the reported data. The failure torque was slightly lower for the case with ligament laxity (9.4 Nm, 70.3°) and demonstrated a higher rotation at failure.

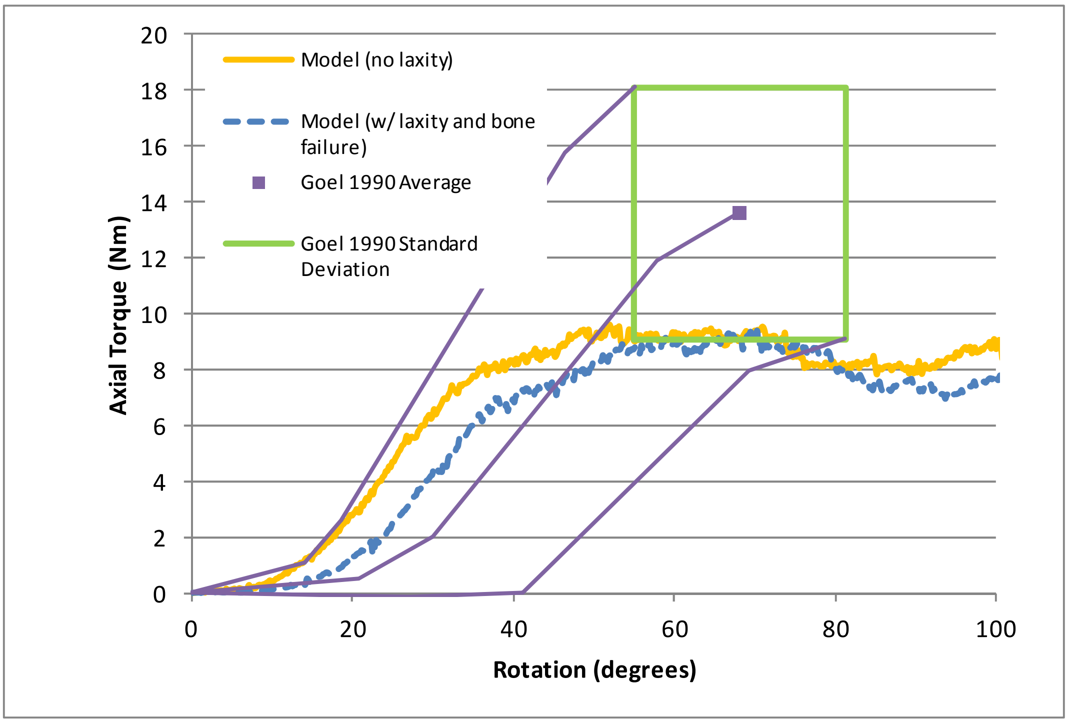

Fig. 6. Axial torque versus rotation

IV. Discussion

The model development phase of this work included several pre-studies to define appropriate boundary conditions to reproduce the experimental tests. It was noted that a precise application and reproduction of the boundary conditions was necessary to use the experimental results for model validation. The extension load case was found to be particularly sensitive to the boundary conditions such as the location where the load was applied. In addition, due to the large rotations encountered during the distractions, geometric nonlinearity was found to be important. This included the load path of some ligaments, which could pass through other tissues under large deformations leading to lower than expected moments in flexion and extension loading.

Under axial rotation, Goel et al. [9] reported a bi-linear response for the torque-rotation relationship, with very little torque (on the order of 0.5 Nm) up to rotations of approximately 20 degrees. Failure occurred by rupture of the C1-C2 joint capsular ligament and PAAM. The model predicted ligament failure and distraction of the C1-C2 joint while most other ligaments remained intact as reported by Goel et al.; however, the axial torque required for relatively low rotations, on the order of 20° (Fig. 6), was higher than measured experimentally. Since much of the rotation was reported to occur between C1 and C2, particularly at low angles, [9] this difference was attributed to the lack of laxity in the related ligaments. Based on these findings, the rotation case was used for an initial study to investigate ligament laxity. When the laxity of the capsular ligaments between C1 and C2 was increased significantly, it was found that the AAAM and PAAM ligaments still provided a significant resistance to rotation. Adding a laxity of 1 mm to these ligaments reduced this torque by approximately 0.5 Nm so that the rotation primarily occurred in the joint between C1 and C2. The increased laxity did not have a significant effect on the segment response with the exception of a reduced moment in flexion and significant increase in angle for the axial rotation case (Fig. 7). Several additional laxity scenarios were considered for the C1-C2 capsular ligaments and it was found that a laxity beyond 1mm did not provide significant benefit in terms of improving the rotation response without adversely affecting the flexion and extension cases. As expected, introducing symmetric anterior-posterior laxity did not affect the tension results significantly. This preliminary study demonstrated that laxity needs to be considered for the upper cervical spine and that all of the responses are interrelated.

The as-measured ligament properties implemented in the upper cervical spine model provided reasonable estimates of the failure load (Fig. 8) and distraction. The predicted failure load in tension was higher than reported experimentally and was attributed to the increased stiffness and strength of the ligaments [5] used in this study; however, the initial response of the model was stiffer than that measured experimentally (Fig. 5).

Because the tension case was relatively simple in terms of loading, this was attributed to the experimental boundary conditions or preconditioning of the test sample and any ligament laxity not included in the numerical model. Introducing a limited amount of laxity offset the response as expected and did not significantly change the ultimate load. The tissues where failure initiated were consistent with the observed failure locations in the literature. In tension loading, Dibb [8] reported failures as complete joint disruption, specifically the posterior ligaments. A small number of hard tissue failures included Type III dens fracture, some C2 lamina fractures and failure at the fixation. No bony or hard tissue failures were observed in the model for the tension case.

The predicted moment at failure in flexion was lower when laxity and bone failure were included (Fig. 8), and was primarily due to an odontoid fracture. Although this was observed in the experimental testing, the predicted Type II odontoid fracture (compared to a Type III fracture in the experiments) indicates that local geometric differences such as bone geometry and cortical shell thickness should be investigated further. The extension results were consistent for both cases.

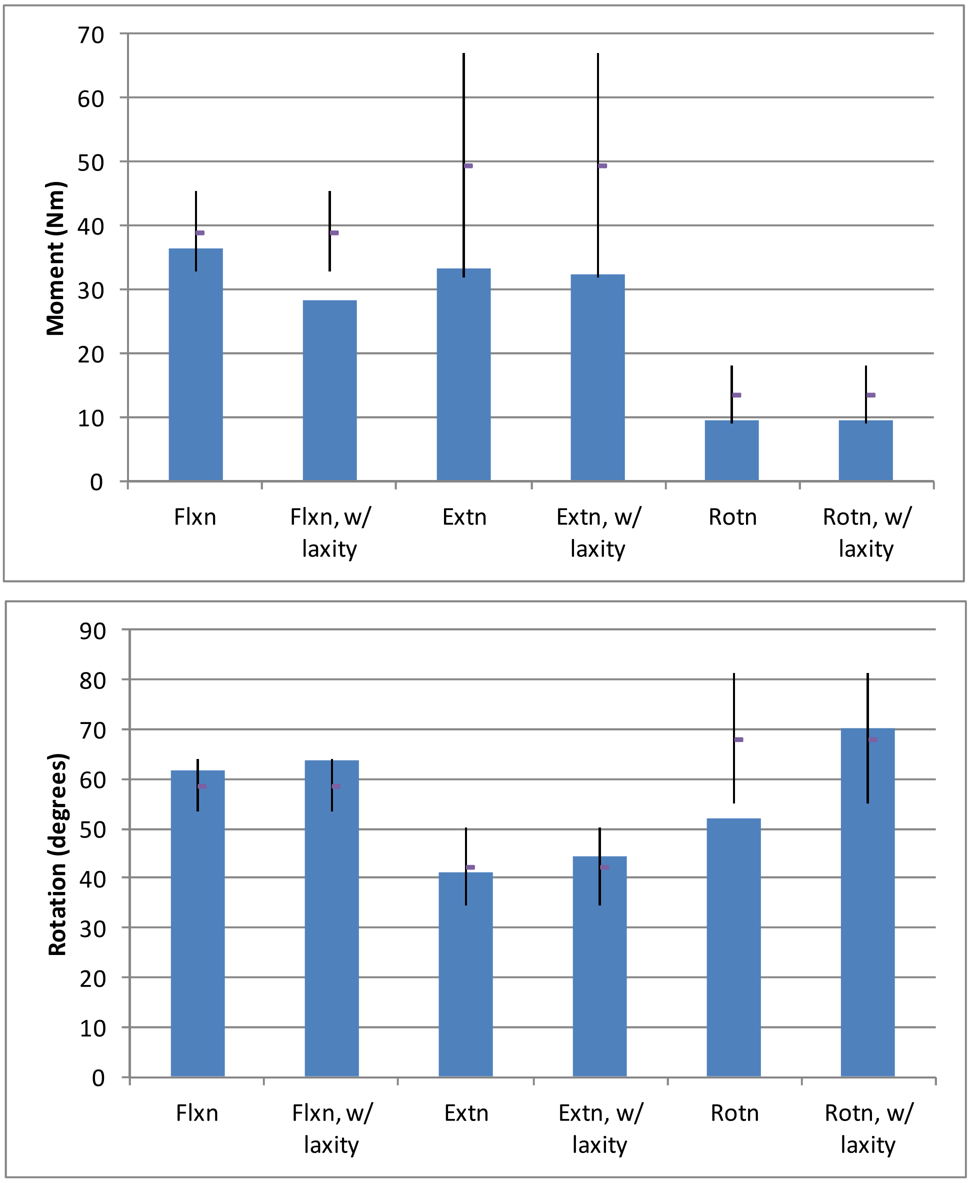

Fig. 7. Comparison of predicted versus measured failure values for flexion, extension and rotation

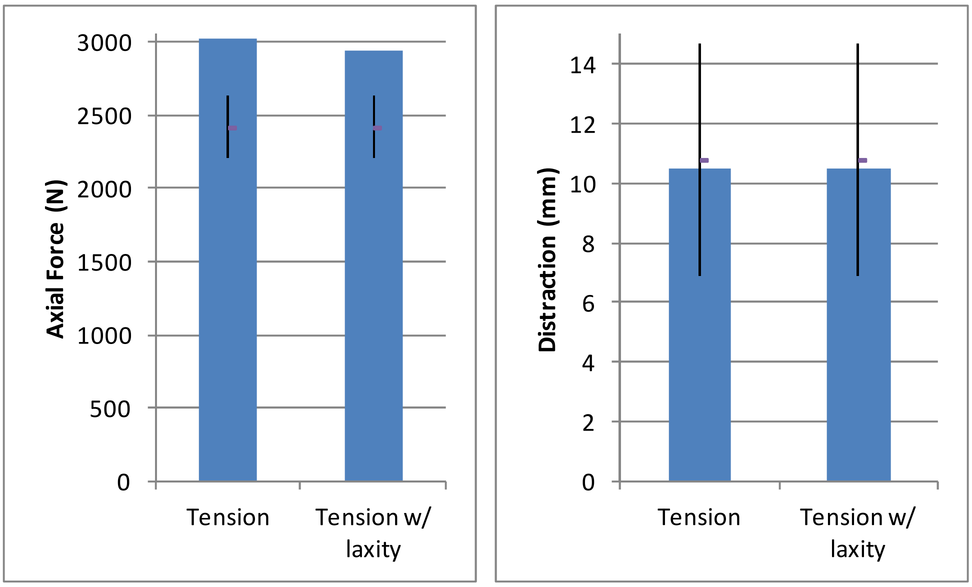

Fig. 8. Comparison of predicted versus measured failure values for tension loading

V. CONCLUSIONS

In general, the finite element upper cervical spine model was able to predict ultimate failure loads, moments and distractions for the investigated modes of loading in agreement with the available experimental data. The ultimate load in tension was higher than the experimental average due to the younger ligament properties used in the model, compared to those in the older experimental test samples. The predicted failure moments for flexion and extension were within the experimental corridors, but lower than the average value, which was attributed to geometric nonlinearity and possible early facture of the vertebrae due to the local tissue geometry. Some limitations were noted including the potential for vertebral failure at large rotations in flexion and extension, and the higher initial stiffness predicted by the model compared to the experimental results. These issues were addressed, in part, through laxity in some ligaments but require further study. Unfortunately, detailed information on ligament laxity is not available in the literature. Future work will investigate optimization approaches to provide improved estimates of the upper cervical spine response and failure.

The current study was limited to an isolated functional spinal unit model, but provides validation not previously addressed using a detailed model of the upper cervical spine. A next step is to integrate these results into an existing full cervical spine model to investigate injury under more representative loading conditions. The current model does not directly consider spinal cord or nerve root injury, which could be inferred by the deformation of the surrounding structures and tissues.

VI. ACKNOWLEDGEMENT

The authors gratefully acknowledge the support of the Global Human Body Model Consortium. The authors thank Yibing Shi and Zine Ben Aoun for reviewing the manuscript and providing valuable feedback.

VII. REFERENCES

[1] Panzer, M.B., Fice, J.B., Cronin, D.S., Cervical Spine Response in Frontal Crash, *Medical Engineering & Physics*, Volume 33, Issue 9, November 2011, Pages 1147-1159.

[2] Fice, J.B., Cronin, D.S., 2012. Investigation of whiplash injuries in the upper cervical spine using a detailed neck model, *Journal of Biomechanics*, doi:10.1016/j.jbiomech.2012.01.016.

[3] Cusick, J.F., and Yoganandan, N., 2002. Biomechanics of the Cervical Spine 4: Major Injuries. *Clinical Biomechanics*, 17, 1 – 20.

[4] Fice, J., Moulton, J., Cronin, D.S., Development of a Detailed Finite Element Neck Model for Automotive Safety Research, *Thirty-Ninth International Workshop on Human Subjects for Biomechanical Research*, Dearborn, MI, November 6, 2011.

[5] Mattucci, S., Cronin, D., Chandrashekar, N., Moulton, J., Mechanical Properties of Human Craniovertebral Ligaments, *American Society of Biomechanics*, August 2011, California.

[6] Gayzik FS, Moreno DP, Geer CP, Wuertzer SD, Martin RS, Stitzel JD. Development of a full body CAD dataset for computational modeling: a multi-modality approach. *Ann Biomed Eng.* 2011; 39(10):2568-2583.

[7] DeWit, J.A., Cronin, D.S., Cervical Spine Segment Finite Element Model for Traumatic Injury Prediction, *Journal of the Mechanical Behavior of Biomedical Materials*, Accepted Feb 22, 2012.

[8] Dibb, A.T., Nightingale, R.W., Luck, J.F., Chancey, V.C., Fronheiser, L.E., and Myers, B.S., 2009. Tension and Combined Tension-Extension Structural Response and Tolerance Properties of the Human Male Ligamentous Cervical Spine. *Journal of Biomechanical Engineering* 131, 1 – 10.

[9] Goel, V.K., Winterbottom, J.M., Schulte, K.R., Chang, H., Gilbertson, L.G., Pudgil, A.G., and Gwon, J.K., 1990. Ligamentous Laxity Across C0-C1-C2 Complex: Axial Torque-Rotation Characteristics Until Failure. *Spine* 15(10), 990 – 996.

[10] Nightingale, R.W., Chancey, V.C., Ottaviano, D., Luck, J.F., Tran, L., Prange, M., and Myers, B.S., 2007. Flexion and Extension Structural Properties and Strengths for Male Cervical Spine Segments. *Journal of Biomechanics* 40(3), 535 – 542.

[11] McElhaney, J.H., 1966. Dynamic Response of Bone and Muscle Tissue. *Journal of Applied Physiology* 21, 1231 – 1236.

[12] Keaveny, T.M., Morgan, E.F., Niebur, G.L., and Yeh, O.C., 2001. Biomechanics of Trabecular Bone. *Annual Review of Biomedical Engineering* 3, 307 – 333.

[13] Lindahl, O., 1976. Mechanical Properties of Dried Defatted Spongy Bone. *Acta Orthopaedica Scandinavica* 47, 11 – 19.